Materials Transactions, Vol. 48, No. 9 (2007) pp. 2445 to 2448

New TiZrCuPd Quaternary Bulk Glassy Alloys with Potential of Biomedical Applications

S. L. Zhu[1,*], X. M. Wang[1], F. X. Qin[1], M. Yoshimura[2] and A. Inoue[1]

[1]*Institute for Materials Research, Tohoku University, Sendai 980-8577, Japan*
[2]*Materials and Structures Laboratory, Tokyo Institute of Technology, Yokohama 226-8503, Japan*

In this paper, we have developed TiZrCuPd quaternary bulk glassy alloys which seem to be favorable for future application as biomaterials because of the absence of toxic elements such as Ni, Al and Be. A series of $(TiZr)_{50}(CuPd)_{50}$ bulk glassy alloys exhibit high glass-forming ability (with critical diameters of 6 and 7 mm) and relatively large supercooled liquid region (ΔT_x) of over 50 K. This alloy system follows the three empirical rules for stabilization of supercooled liquid. The thermal stability of $Ti_{40}Zr_{10}Cu_{36}Pd_{14}$ bulk glassy alloy was also examined in correlation with the origin for the high glass-forming ability. [doi:10.2320/matertrans.MRA2007086]

(Received April 18, 2007; Accepted June 11, 2007; Published August 1, 2007)

Keywords: *TiZrCuPd, bulk glassy alloy, biomaterial, glass-forming ability, crystallization behavior*

1. Introduction

Bulk glassy alloys are promising materials for structural and functional uses owing to their superior properties compared to their crystalline counterparts.[1,2] It is known that these alloys exhibit high hardness, high tensile strength and good fracture toughness. The unique properties of bulk glassy alloys make them extremely attractive for biomedical application. The mechanical deformation behavior of biological materials, which is characterized by high recovery of strain ($\geq$2%) after deformation, is very different from that of common metallic materials.[3] Another problem concerning metallic implants in orthopedic surgery is the mismatch of Young's modulus between the human bone and metallic implants. The bone is insufficiently loaded due to the mismatch, as called "stress-shielding". In general, the Young's moduli of most traditional metallic biomaterials are at least 10–20 times higher than those of hard tissues (below 20 GPa), such as titanium alloys (110 GPa) and stainless steels (210 GPa).[4] From the point of view of the requirements towards the implant materials for hard tissue replacement, a biomaterial with low elastic modulus has been required. The glassy alloys have lower Young's modulus and most uniquely an extremely high elastic limit of 2%. Bulk glassy alloys would be unique in their ability to flex elastically with the natural bending of the bone and so distribute stresses more uniformly. Faster healing rates will result from reduced stress shielding effects while minimizing stress concentrators.

Ti-based alloys are benefiting for biomedical applications because of their low density, excellent biocompatibility and corrosion resistance.[5,6] A number of studies were carried out to obtain better performance of the Ti-based alloys in terms of their biomedical properties, mechanical properties and workability by either modifying the available Ti-based alloys or exploring new compositions.[7–11] The excellent biocompatibility and corrosion resistance of Ti-based alloys are attributed to their surface oxide layer which is mainly composed of TiO_2. Combining the advantage of bulk glass alloy with that of Ti-based crystalline alloy, Ti-based bulk glassy alloys are expected to be applied as a new type of biomaterials. Some papers reported the Ti-rich bulk glassy alloys which had high glass-forming ability. These Ti-rich bulk glassy alloys were developed in the framework of the Ti-Ni-Cu and Ti-Zr-Cu-Ni alloy systems.[12,13] However, the presence of Ni would restrict the biomedical applications of Ti-based bulk glassy alloys because of its cellar toxicity. Since Pd and Ni belong to the same family in an element periodic table, the replacement of Ni by Pd should be considered to eliminate the harmful influence of Ni. In this paper, we developed $(TiZr)_{50}(CuPd)_{50}$ bulk glassy alloys. Glass-forming ability, thermal stability and mechanical properties of the bulk glassy alloys will be presented.

2. Experimental Procedure

Ingots of a series of Ti-Zr-Cu-Pd alloys were prepared by arc-melting the mixtures of the pure elements with purities above 99.9% in an argon atmosphere. The alloy composition represents the nominal atomic percentage of the mixture. The ribbons and cylindrical rods with different diameters were prepared by melt spinning and copper mold casting, respectively. Glassy structure was examined by X-ray diffraction (XRD). Thermal stability was evaluated by differential scanning calorimetry (DSC) and differential thermal analysis (DTA).

3. Results and Discussion

Figure 1 shows the XRD patterns of the as cast $Ti_{50-x}Zr_xCu_{50-x}Pd_x$ ($x = 8$, 10, 12, 14, 16, 18, 20) alloy rods with different diameters. For $x = 8$, 10, 18 and 20, the broadened XRD pattern of the 4 mm rod denotes a glassy nature. For $x = 12$ and 16, a fully glassy state was confirmed for the rod of 6 mm in diameter. The largest critical diameter of 7 mm was obtained for $x = 14$.

In general, a critical cooling rate for glass formation, which is the minimum cooling rate necessary to keep alloy melt without precipitation of crystalline phase down to a glass transition temperature, is used to evaluate the glass-

*Corresponding author, E-mail: slzhu@imr.tohoku.ac.jp

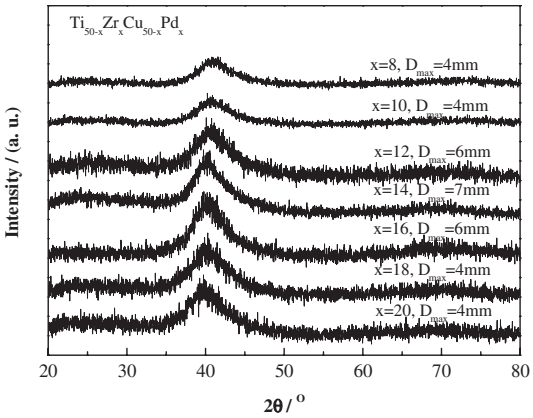

Fig. 1 XRD patterns of $Ti_{50-x}Zr_xCu_{50-x}Pd_x$ glassy alloy rods produced by copper mold casting.

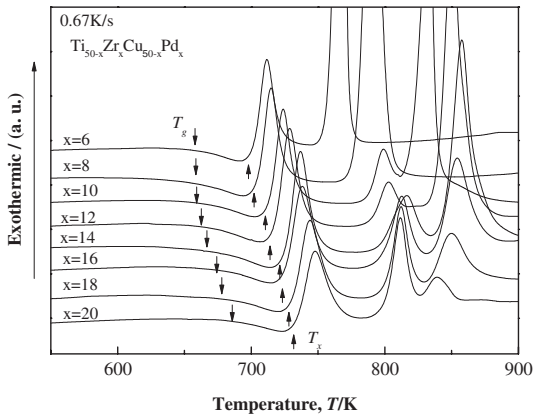

Fig. 3 DSC curves of $Ti_{50-x}Zr_xCu_{50-x}Pd_x$ glassy alloy ribbons produced by melt spinning.

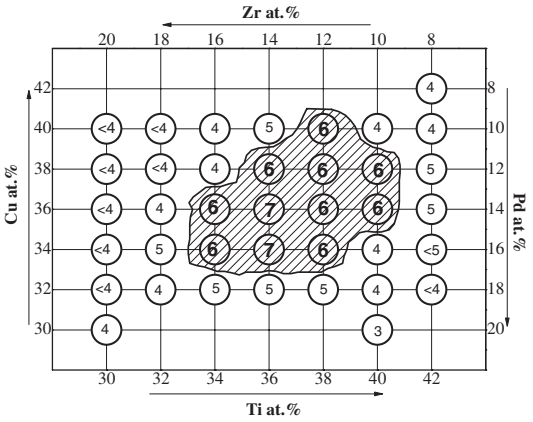

Fig. 2 Critical diameters (mm) of $(TiZr)_{50}(CuPd)_{50}$ glassy alloy rods produced by copper mold casting.

forming ability (GFA) of an alloy. Lower critical cooling rate means higher GFA. However, it is difficult to measure accurately the critical cooling rate. In view of the inverse proportional relation between the cooling rate during solidification and section thickness of cast sample, the maximum diameter of a fully glassy rod sample may be an alternative of GFA. The larger the maximum diameter, the higher is the GFA. Figure 2 shows the critical diameters of $(TiZr)_{50}(CuPd)_{50}$ glassy alloys. In the shadow area, the critical diameters are larger than 5 mm. Especially for $Ti_{36}Zr_{14}Cu_{36}Pd_{14}$ and $Ti_{36}Zr_{14}Cu_{34}Pd_{16}$ alloy, a full glassy structure can be obtained in the rod samples with diameter up to 7 mm. To our knowledge from the reported data, the rod diameter of 6 mm is the largest for Ti-based glassy alloys without Be.[14] In the present study, a series of 6 mm Ti-based glassy alloys were produced and the largest critical diameter was 7 mm. This indicates that the present alloy system has higher glass-forming ability than those of the former Ti-based alloys.

Little is known about the glass formation tendency of Ti-Zr-Cu-Pd quaternary alloy system, though some studies have been made for Ti-Zr-Cu-Ni alloy system.[12,13] Since Pd and Ni belong to the same family in a periodic table, these studies can be referenced. According to conventional nucleation theory, GFA can be evaluated by considering the competition between a decreasing nucleation barrier and an increasing viscosity with decreasing temperature of supercooled liquid. The three empirical component rules of multicomponent system, significant different atomic sizes among the constituent elements and large negative heats of mixing, have been cited and used to interpret the GFA of the present glassy alloys.[15] The atomic radii of Ti, Zr, Cu and Pd are 0.147, 0.16, 0.128 and 0.137 nm, respectively. These large atomic size mismatches can result in significant disorder in structural topology which is large enough to enable the formation of a glassy structure during solidification. Pd in the liquid state has a negative heat of mixing with Cu of -14 kJ/mol and high negative heat of mixing with Zr and Ti of -91 kJ/mol and -65 kJ/mol, respectively.[16] This may cause the formation of chemical short range order or atomic cluster in the supercooled liquid.

Figure 3 shows the DSC curves obtained during continuous heating for various Ti-based glassy alloy ribbons with a heating rate of 0.67 K/s. During heating, all the curves exhibit an endothermic event, characteristic of glass transition to supercooled liquid, followed by exothermic reactions corresponding to crystallization of the supercooled liquid. The alloys exhibit two or three exothermic events due to multi-stage crystallization depending on alloy composition. The onset temperature of the first exothermic peak is assumed to be the crystallization temperature (T_x) of each glassy phase. All the characteristic temperatures are also marked with arrows in Fig. 3. T_g and T_x shift to higher temperatures with increasing Pd content. Figure 4 shows the DTA curves obtained during continuous heating for various master alloys with a heating rate of 0.33 K/s. The onset melting temperature (T_m), and liquidus temperature (T_l) are shown by arrows in Fig. 4. T_m shows a slight change with increasing Pd and Zr contents. However, T_l decreases firstly, and then increases as Pd and Zr are over 14%. Several parameters have been used to evaluate the GFA of glassy alloys. The reduced glass transition temperature (T_{rg}) defined as the ratio of T_g to T_l has been successfully used to evaluate the GFA of various glassy alloys. The supercooled liquid (SCL) region, defined as the temperature interval $\Delta T_x (= T_x - T_g)$, has also been regarded as a useful parameter of GFA.[17] The other GFA parameter $\gamma = \frac{T_x}{T_g + T_l}$ was recently proposed to predict the GFA for various glassy

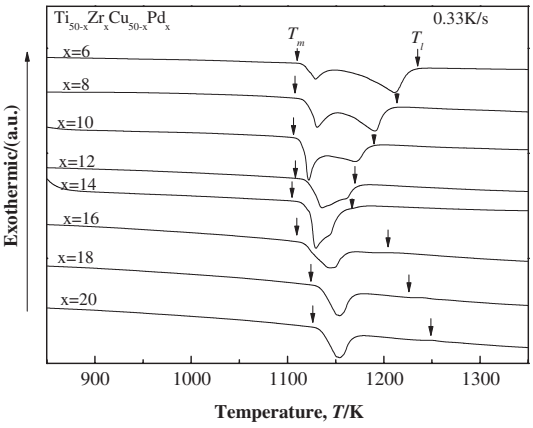

Fig. 4 DTA curves of $Ti_{50-x}Zr_xCu_{50-x}Pd_x$ master alloys.

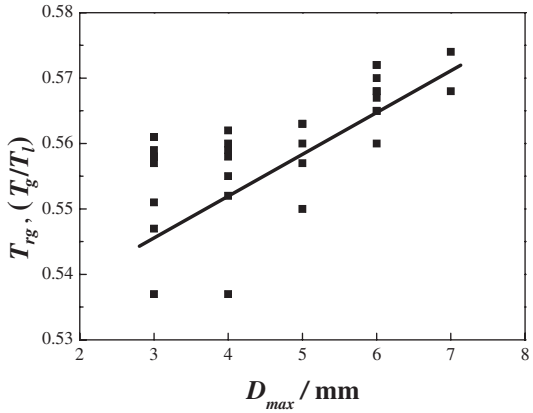

Fig. 5 Relation between reduced glass transition temperature (T_{rg}) and maximum diameters (D_{max}) for $(TiZr)_{50}(CuPd)_{50}$ bulk glassy alloys.

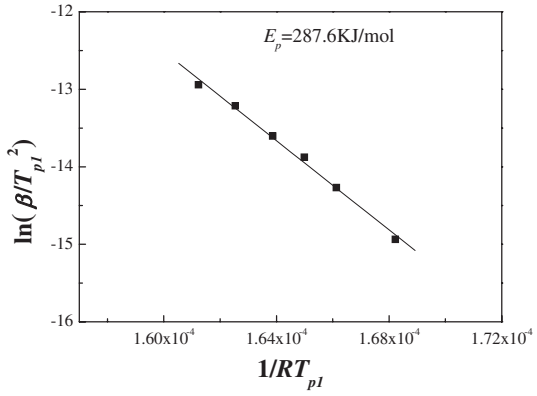

Fig. 6 Kissinger plot of a $Ti_{40}Zr_{10}Cu_{36}Pd_{14}$ glassy alloy.

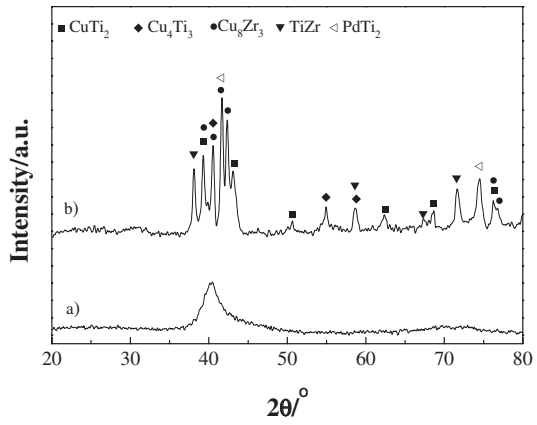

Fig. 7 XRD patterns of $Ti_{40}Zr_{10}Cu_{36}Pd_{14}$ glassy alloy ribbons subjected to heat treatment at a) 750 K and b) 900 K.

alloy systems.[18] For the present alloy system, only T_{rg}, which reflects the difficulty of nucleation of crystalline phase from supercooled liquid, can correspond to the glass-forming ability. Figure 5 shows the relationship between T_{rg} and critical diameters for the TiZrCuPd alloys. The alloys with larger critical diameters tend to have higher T_{rg}. But the other parameters cannot suit to this quaternary alloy system.

The Kissinger method is used to determine the kinetic constants of phase transformations obtained using a DSC. The Kissinger method can be described briefly as following equation:[19]

$$-\frac{E_p}{R} = d\left(\ln\frac{\beta}{T_p^2}\right) \Big/ d\left(\frac{1}{T_p}\right),$$

where β is the heating rate, T_p is the first peak temperature, R is gas constant and E_p is the activation energy. The plot of $\ln(\frac{\beta}{T_p^2})$ versus $\frac{1}{T_p}$ has a linear shape, which allows E_p to be calculated using the slope of the linear fit. Figure 6 shows the plot of $\ln(\frac{\beta}{T_p^2})$ versus $\frac{1}{T_p}$ for the $Ti_{40}Zr_{10}Cu_{36}Pd_{14}$ glassy alloy. The activation energy E_p is 287.6 kJ/mol, which is similar to those of $Zr_{55}Cu_{30}Al_{10}Ni_5$ glassy alloy (278 kJ/mol)[20] and $Ti_{41.5}Zr_{2.5}Hf_5Cu_{42.5}Ni_{7.5}Si_1$ glassy alloy (284 kJ/mol),[21] indicating high thermal stability for crystallization.

Figure 7 shows XRD patterns of the $Ti_{40}Zr_{10}Cu_{36}Pd_{14}$ glassy ribbons subjected to annealing. The annealing process was conducted by using a DSC at a heating rate of 0.67 K/s. Heating was stopped at a) 750 K (after the first exothermic peak) and b) 900 K (after the second exothermic peak), respectively. The XRD pattern of the alloy annealed at 750 K does not show any sharp diffraction peak, suggesting that nano-crystallization has occurred. The residual glassy phase would transform into some intermetallics at higher temperatures. The phases of $CuTi_2$, Cu_8Zr_3, Cu_4Ti_3, TiZr and $PdTi_2$ can be simultaneously indexed in the XRD pattern.

4. Conclusion

We have investigated the glass-forming ability of TiZrCuPd quaternary alloy system, which are expected to be applied as biomaterials because of the absence of toxic elements such as Ni, Al and Be. A series of $(TiZr)_{50}(CuPd)_{50}$ bulk glassy alloys exhibit high glass-forming ability (with critical diameters of 6 and 7 mm) and relatively large supercooled liquid region (ΔT_x) of over 50 K. The $Ti_{40}Zr_{10}Cu_{36}Pd_{14}$ bulk glassy alloy has high activation energy of 287.6 KJ/mol for crystallization, indicating that the Ti-based glassy alloy has high thermal stability against crystallization. The first crystallization peak in the DSC curve corresponds to the precipitation of nanocrystalline phase. Five phases of $CuTi_2$, Cu_8Zr_3, Cu_4Ti_3, TiZr and $PdTi_2$ can be indexed for the alloy subjected to complete crystallization. The present bulk glassy alloy seems to be favorable for future application as biomaterials.

REFERENCES

1) A. Inoue and A. Takeuchi: Mater. Trans. **43** (2002) 1892–1906.
2) A. Inoue: Acta Mater. **48** (2000) 279–306.
3) B. Y. Li, L. J. Rong and Y. Y. Li: Intermetallics **8** (2000) 643–646.
4) J. A. Helsen and H. J. Breme: *Metals as biomaterials*, (Wiley, Baffins Lane, Chichester, England, 1998).
5) M. Niinomi: Matall. Mater. Trans. **33A** (2002) 477–486.
6) R. V. Noort: J. Mater. Sci. **22** (1987) 3801–3811.
7) Y. L. Cai, C. Y. Liang, S. L. Zhu, Z. D. Cui and X. J. Yang: Scrip. Mater. **54** (2006) 89–92.
8) D. Kuroda, M. Niinomi, M. Morinaga, Y. Kato and T. Yashiro: Mater. Sci. Eng. A: Prop. Microstruct. Process. **243** (1998) 244–249.
9) S. L. Zhu, X. J. Yang, D. H. Fu, L. Y. Zhang, C. Y. Li and Z. D. Cui: Mater. Sci. Eng. A **408** (2005) 264–268.
10) G. He, J. Eckert, Q. L. Dai, M. L. Sui, W. Löser, M. Hagiwara and E. Ma: Biomaterials **24** (2003) 5115–5120.
11) C. X. Cui, H. Liu, Y. C. Li, J. B. Sun, R. Wang, S. J. Liu and A. L. Greer: Mater. Lett. **59** (2005) 3144–3148.
12) X. H. Lin and W. L. Johnson: J. Appl. Phys. **78** (1995) 6514–6519.
13) C. C. Hay and S. C. Glade: Appl. Phys. Lett. **80** (2002) 3096–3098.
14) S. L. Zhu, X. M. Wang, F. X. Qin. and A. Inoue: Mater. Sci. Eng. A **459** (2007) 233–237.
15) A. Inoue, T. Zhang and T. Masumoto: J. Non-Cryst. Solids **473** (1993) 156–158.
16) A. Takeuchi and A. Inoue: Mater. Trans. JIM **41** (2000) 1372–1378.
17) A. Inoue: Mater. Trans. JIM **36** (1995) 866–875.
18) Z. P. Lu and C. T. Liu: Acta Mater. **50** (2002) 3501–3512.
19) H. E. Kissinger: J. Res. Natl. Bur. Stand., Sect. A **57** (1956) 217–221.
20) S. L. Zhu, X. M. Wang, F. X. Qin and A. Inoue: Intermetallics **15** (2007) 885–890.
21) Y. J. Huang, J. Shen, J. F. Sun and X. B. Yu: J. Alloys Compd. **427** (2007) 171–175.